



Original Article

PCSK9 and APOA4: The Dynamic Duo in TMAO-induced Cholesterol Metabolism and Cholelithiasis



Chao Shi^{1,2,3#}, Jingjing Yu^{1,2#}, Ziang Meng^{1,2#}, Dongxu Lu^{1,2}, Haoran Ding^{1,2}, Haijun Sun^{1,3}, Guangxin Shi⁴, Dongbo Xue^{1,2} and Xianzhi Meng^{1,2*}

¹Department of General Surgery, The First Affiliated Hospital of Harbin Medical University, Harbin, Heilongjiang, China; ²Key Laboratory of Hepatosplenic Surgery, Ministry of Education, The First Affiliated Hospital of Harbin Medical University, Harbin, Heilongjiang, China; ³Ambulatory Surgery Center, The First Affiliated Hospital of Harbin Medical University, Harbin, Heilongjiang, China; ⁴Department of Internal Medicine, The Third Hospital of Changtu County, Tieling, Liaoning, China

Received: November 05, 2024 | Revised: December 31, 2024 | Accepted: January 22, 2025 | Published online: February 11, 2025

Abstract

Background and Aims: Cholesterol synthesis and gallstone formation are promoted by trimethylamine-N-oxide (TMAO), a derivative of trimethylamine, which is a metabolite of gut microbiota. However, the underlying mechanisms of TMAO-induced lithogenesis remain incompletely understood. This study aimed to explore the specific molecular mechanisms through which TMAO promotes gallstone formation. **Methods:** Enzyme-linked immunosorbent assays were used to compare serum concentrations of TMAO, apolipoprotein A4 (APOA4), and proprotein convertase subtilisin/kexin type 9 (PCSK9) between patients with cholelithiasis and normal controls. A murine model of TMAO-induced cholelithiasis was employed, incorporating assays of gallstone weight and bile cholesterol content, along with RNA sequencing of murine hepatic tissue. A TMAO-induced AML12 hepatocyte line was constructed and transfected with targeted small interfering RNAs and overexpression plasmids. *In vivo* and *in vitro* experiments were performed to determine the expression and regulation of genes related to cholesterol metabolism. **Results:** Serum TMAO and PCSK9 levels were elevated, whereas APOA4 levels were reduced in patients with cholelithiasis. Furthermore, our murine model demonstrated that TMAO upregulated hepatic expression of PCSK9, 3-hydroxy-3-methylglutaryl-CoA reductase, and ATP-binding cassette sub-family G member 5/8, while reducing APOA4 expression, thereby modulating cholesterol metabolism and promoting lithogenesis. PCSK9 and APOA4 were identified as key regulatory genes in the cholesterol metabolic pathway. PCSK9 knockdown increased APOA4 expression, while APOA4 overexpression led to reduced PCSK9 expression. **Conclusions:** TMAO upregulated hepatic PCSK9 expression and reduced APOA4 expression, initiating a feedback loop that dysregulated cholesterol metabolism and promoted lithogenesis.

Citation of this article: Shi C, Yu J, Meng Z, Lu D, Ding H, Sun H, et al. PCSK9 and APOA4: The Dynamic Duo in TMAO-induced Cholesterol Metabolism and Cholelithiasis. J Clin Transl Hepatol 2025;13(4):295–305. doi: 10.14218/JCTH.2024.00403.

Introduction

Cholelithiasis is a highly prevalent disorder of the digestive system, afflicting 6% of adults worldwide.¹ Its incidence is increasing, particularly among females and South Americans. Cholesterol gallstones are the leading subtype.

Trimethylamine-N-oxide (TMAO) is synthesized by the hepatic enzyme flavin-containing monooxygenase 3 (FMO3) from the substrate trimethylamine, which is produced by the gut microbiota through the conversion of dietary phosphatidylcholine, choline, L-carnitine, and betaine.² TMAO has been implicated in the pathogenesis of cardiovascular diseases, including hypertension,³ atherosclerosis,⁴ coronary heart disease,⁵ stroke,⁶ and abdominal aortic aneurysm⁷; it is also established as a risk factor for metabolic disorders such as obesity,⁸ type 2 diabetes,⁹ osteoporosis,¹⁰ graft-versus-host disease,¹¹ and chronic kidney disease.¹² Additionally, proline/serine-rich coiled-coil protein 1 deficiency may increase FMO3 expression, thereby upregulating TMAO production.¹³ TMAO binds and activates endoplasmic reticulum stress kinase, inducing the transcription factor FOXO1, which exacerbates metabolic dysfunction and atherosclerosis.¹⁴

The relationship between gut microbiota and lithogenesis has garnered increasing attention. Certain bacterial species not only affect bile microenvironment but also actively participate in lithogenesis by producing enzymes such as β -glucuronidase and mucins that influence bile acid and cholesterol metabolism.^{15,16} However, the underlying mechanisms of TMAO's role in promoting lithogenesis remain unclear.

We utilized RNA sequencing, bioinformatic approaches, and both *in vivo* and *in vitro* experiments to confirm that TMAO promotes cholelithiasis by dysregulating hepatic cholesterol metabolism through its effects on the key regulatory genes apolipoprotein A4 (APOA4) and proprotein convertase subtilisin/kexin type 9 (PCSK9).

Keywords: TMAO; Cholesterol metabolism; Cholelithiasis; PCSK9; APOA4; Feedback loop.

[#]Contributed equally to this work.

*Correspondence to: Xianzhi Meng, Department of General Surgery, The First Affiliated Hospital of Harbin Medical University, Harbin, Heilongjiang 150001, China. ORCID: <https://orcid.org/0000-0003-3409-4693>. Tel: +86-451-85555883, E-mail: mengxianzhi@hrbmu.edu.cn.

Methods

Clinical sample collection

Serum samples were collected from ten patients with asymptomatic cholelithiasis undergoing cholecystectomy (gallstone disease group, GSD group). Exclusion criteria included histories of: antibiotic or probiotic treatment within three months prior to sample collection; other digestive tract-related diseases; allergies or autoimmune diseases or ongoing immunomodulatory therapy; neurological or neurodevelopmental disorders or chronic pain syndromes; obesity based on a body mass index ≥ 30 kg/m²; metabolic syndrome or severe malnutrition; malignancy or ongoing cancer treatment; vegetarian diet; and fecal microbiota transplantation. For comparison, serum samples from 10 healthy liver transplant donors were included as a negative control (NC) group, using the same inclusion and exclusion criteria. After extraction, samples were promptly transported in liquid nitrogen and stored long-term at -80°C .

Animal experiments

Male C57BL/6J mice (six to eight weeks old, non-siblings), weighing 20–22 grams, were purchased from Liaoning Changsheng Biotechnology Co., Ltd. (Liaoning Province, China). All mice were maintained on a 12 h light/dark cycle at 22°C , with unrestricted access to standard rodent chow and water, and were housed under pathogen-free conditions. Mice were allowed to acclimatize for one week before experiments. All animal experiments were approved by the Animal Ethics Committee of The First Affiliated Hospital of Harbin Medical University. We employed a murine model of cholelithiasis induced by a lithogenic diet. Mice were fed either normal diet (ND, containing 0.02% cholesterol) or a lithogenic diet (LD, containing 1.25% cholesterol, 15% total fat, and 0.5% cholic acid) for four weeks.¹⁷ To investigate the effects of TMAO administration, 30 mice were randomly divided into three groups (NC, LD, and LD+TMAO), with each group housed separately. Mice in the NC group received an intraperitoneal injection of 200 μL saline as a control after 1 week. Mice in the LD group received an intraperitoneal injection of 200 μL saline for four consecutive weeks after 1 week. Mice in the LD+TMAO group received intraperitoneal injections of 200 μL TMAO (20 mg/kg/day, Sigma-Aldrich, St. Louis, MO, USA) for four consecutive weeks after 1 week.¹⁸ To investigate the effects of TMAO inhibition on lithogenesis, 20 mice were randomly divided into two groups, with each group housed separately. Mice in both groups received the LD, while the intervention group received LD+1% 3,3-dimethyl-1-butanol (DMB, Sigma-Aldrich, St. Louis, MO, USA), an inhibitor of TMAO synthesis, added to their drinking water.¹⁹

Measurement of gallstones and bile components

Mice were fasted for 6 h but allowed free access to water. Following euthanasia, the presence or absence of gallstones was determined. Gallbladders were removed intact, and all contents were extracted and placed on a glass dish to allow complete evaporation of liquid content. The residual solid mass was weighed.

We conducted a separate experiment following the methodology described by Matsumoto *et al.*²⁰ Mice were anesthetized with isoflurane and maintained at 37°C on a heating pad. The common bile duct was ligated and cannulated with a PE-10 catheter to collect bile for 120 min, during which time the flow rate was measured. Total cholesterol (catalog number A111-1-1) and total bile acids (catalog

number E003-2-1) were assayed according to the manufacturer's instructions (Nanjing JIANCHENG Bioengineering, Nanjing, China). Phospholipid concentrations were quantified using a Wako kit (catalog number 296-63801, Osaka, Japan), also following the manufacturer's instructions. Activity levels were measured using a multi-mode microplate reader (BioTek Synergy NEO).

Calculation of cholesterol saturation index (CSI)

The CSI of bile was calculated using the method proposed by Carey *et al.*²¹ The steps were as follows: (1) Calculation of the molar percentages (mol%) of cholesterol, bile acids, and phospholipids based on their molecular weights. (2) Calculation of the ratio of phospholipids to the sum of phospholipids and bile acids. (3) Using the ratio obtained in the previous step, reference the Carey table to obtain the theoretical molar percentage concentration of cholesterol. (4) $\text{CSI} = \text{actual molar percentage concentration of cholesterol} / \text{theoretical molar percentage concentration of cholesterol}$.

RNA sequencing

Three mice were randomly selected from each group and underwent partial hepatectomy to harvest liver tissue for RNA sequencing. cDNA libraries were sequenced on the Illumina sequencing platform by Wuhan Metware Biotechnology Co., Ltd. RNA was extracted using the Trizol method, dissolved in 50 μL of diethyl pyrocarbonate-treated water,²² and qualified and quantified using a Qubit Fluorometer and a Qsep400 high-throughput biological fragment analyzer. Raw data were filtered using fastp, and gene alignment was calculated using featureCounts.²³ The fragments per kilobase of transcript per million fragments mapped (hereinafter referred to as FPKM) value of each gene was calculated based on its length.

Enzyme-linked immunosorbent assay (ELISA)

Serum samples from 10 GSD and 10 NC patients, as well as from mice in the LD and LD+DMB groups, were subjected to ELISA testing. ELISA kits for measuring human TMAO, PCSK9, APOA4, and murine TMAO were obtained from Lptech (China) and used according to the manufacturer's instructions. The absorbance of the samples was read at 450 nm using a microplate reader (Multiskan-FC, Thermo Scientific).

Immunohistological analysis

Immunohistological analysis, tissue preparation, mounting, and blocking were conducted as previously described.²⁴ Paraffin-embedded tissue sections were incubated overnight at 4°C with antibodies against APOA4 (Proteintech, China), 3-hydroxy-3-methylglutaryl-CoA reductase (HMGR) (CUS-ABIO, China), ATP-binding cassette sub-family G member 5 (ABCG5) (Abmart, China), PCSK9, and ATP-binding cassette sub-family G member 8 (ABCG8) (Abclonal, China). After PBS washing, the sections were incubated with secondary antibodies for 1 h at room temperature, followed by counterstaining with hematoxylin and eosin. Histological sections were incubated with primary antibodies overnight at 4°C . After thorough washing with PBS, CoraLite 594 Goat Anti-Rabbit IgG (Proteintech, China) was applied and incubated for 1 h at room temperature. The slides were then stained with 4',6-diamidino-2-phenylindole (SEVEN, China) and observed under a fluorescence microscope.

Cell culture and treatment

The murine normal hepatocyte line AML12 was acquired from

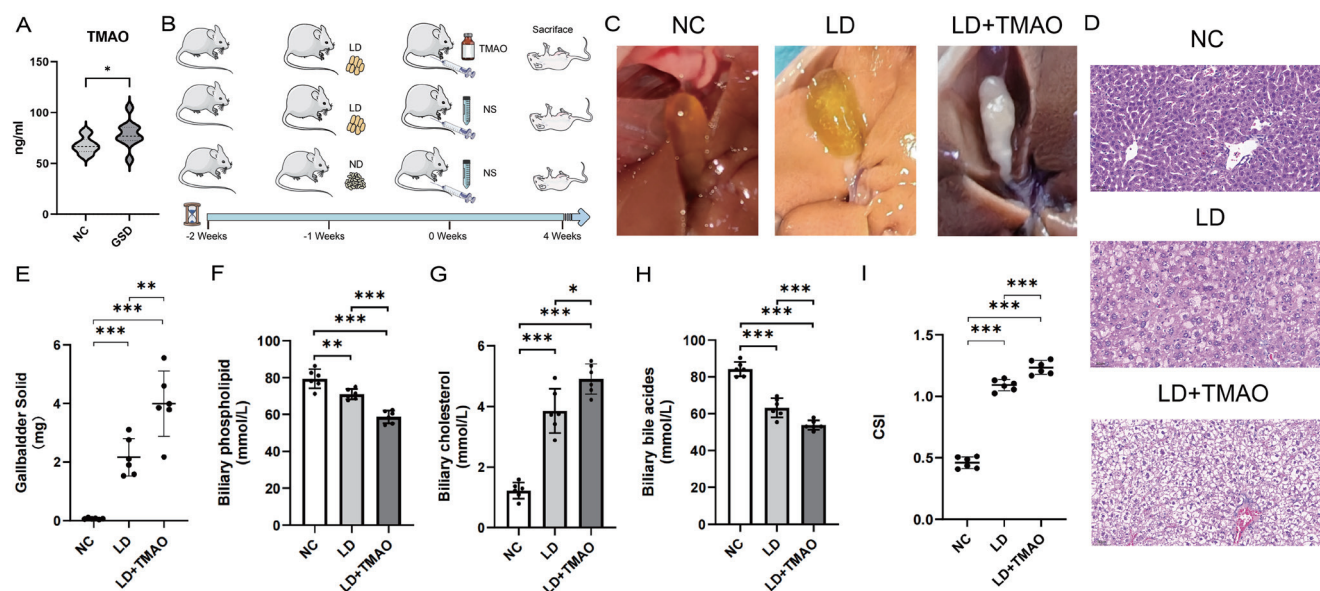


Fig. 1. Effects of TMAO on cholesterol metabolism and lithogenesis in mice. (A) Serum TMAO concentrations in patients with cholelithiasis and the control group. (B) Overview of the experimental process. (C) Gallstone formation in the NC, LD, and LD+TMAO groups. (D) Hematoxylin and eosin staining of murine hepatic tissue. (E) Weights of solid intracystic contents in each group. (F) Phospholipid concentration in murine bile. (G) Cholesterol concentration in murine bile. (H) Bile acid concentration in murine bile. (I) CSI values in each group. Data are expressed as mean \pm SEM ($n = 6$ per group). * $p < 0.05$, ** $p < 0.01$, and *** $p < 0.001$. NC, Negative control; LD, lithogenic diet; LD+TMAO, LD + Trimethylamine N-oxide. NC, negative control; GSD, gallstone disease; LD, lithogenic diet; TMAO, trimethylamine-N-oxide; CSI, calculation of cholesterol saturation index.

Cyagen Biosciences Inc. (Shanghai, China) and cultured using AML12 cell-specific culture medium (Procell, Wuhan). AML12 cells were categorized into the following groups, analogous to those used in previous studies⁴: (1) Control (treated with complete culture medium only); (2) TMAO (50 μ M of TMAO); (3) TMAO+APOA4^{OE} (50 μ M of TMAO and APOA4 overexpression); (4) TMAO+PCSK9^{si} (50 μ M of TMAO and PCSK9 inhibition); (5) APOA4^{OE} (APOA4 overexpression); (6) PCSK9^{si} (PCSK9 inhibition).

Plasmid and small interfering RNA (siRNA) transfection

Targeting siRNAs and overexpression plasmids were designed and synthesized by Hanbio Biotechnology (Shanghai, China). Cells were seeded in 6-well plates at a density of 2×10^5 cells per well and cultured overnight until they reached 50–70% confluence. Lipofectamine 2000 (Invitrogen, USA) was employed to transfect the siRNAs and plasmids into AML12 cells in a serum-free medium following the manufacturer’s instructions.²⁵ Eight hours post-transfection, the cells were transferred to a complete culture medium and further incubated for 24 h. The siRNA sequences are summarized in Supplementary Table 1.

Real-time fluorescence quantitative PCR (qPCR)

Total RNA was extracted from tissues or cells using the RNA extraction kit from Axygen Scientific Inc. (Silicon Valley, USA) and then reverse-transcribed into cDNA using the Toyobo Reverse Transcription Kit. SYBR GREEN reagent was employed to detect the expression of target genes. Real-time-qPCR samples were preheated at 95°C for 10 min, followed by 40 cycles of denaturation at 95°C for 15 s and annealing/extension at 60°C for 1 min.²⁶ GAPDH served as the internal reference gene. Data were analyzed using the $2^{-\Delta\Delta Ct}$ method. Supplementary Table 2 provides detailed information regarding the primers.

Western blot (WB) analysis

Equal amounts of protein samples were separated by sodium dodecyl sulfate polyacrylamide gel electrophoresis and transferred onto a polyvinylidene difluoride membrane. The polyvinylidene difluoride membrane was incubated with the primary antibody overnight at 4°C, washed repeatedly with tris-buffered saline containing Tween 20, and then incubated with the secondary antibody for 1 h at room temperature.²⁷ Proteins were visualized using an Enhanced Chemiluminescence Kit (Millipore Corporation), and quantitative analysis of proteins was performed using ImageJ software.²⁸

Statistical analysis

Bioinformatic analysis was conducted using R software (version 4.0.2). GraphPad Prism 8 was employed for statistical analysis. Continuous data with normal distributions were compared between two groups using the t-test or Mann-Whitney U test. The Kruskal-Wallis test was applied for comparisons between three groups of samples. Spearman correlation analysis was utilized for all correlation analyses. In all statistical analyses, $p < 0.05$ was considered significant (* $p < 0.05$, ** $p < 0.01$, *** $p < 0.0001$).

Results

TMAO promotes lithogenesis by dysregulating hepatic metabolism

Serum TMAO levels were significantly higher in GSD patients compared to the control group (Fig. 1A). Our murine model demonstrated that lithogenesis was more prevalent in LD mice than in NC mice and further elevated in the LD+TMAO group (Fig. 1B, C). DMB treatment reduced serum TMAO levels in LD+TMAO-treated mice to the physiological range observed in human serum (Supplementary Fig. 1). The weight of intracystic solid materials increased significantly after

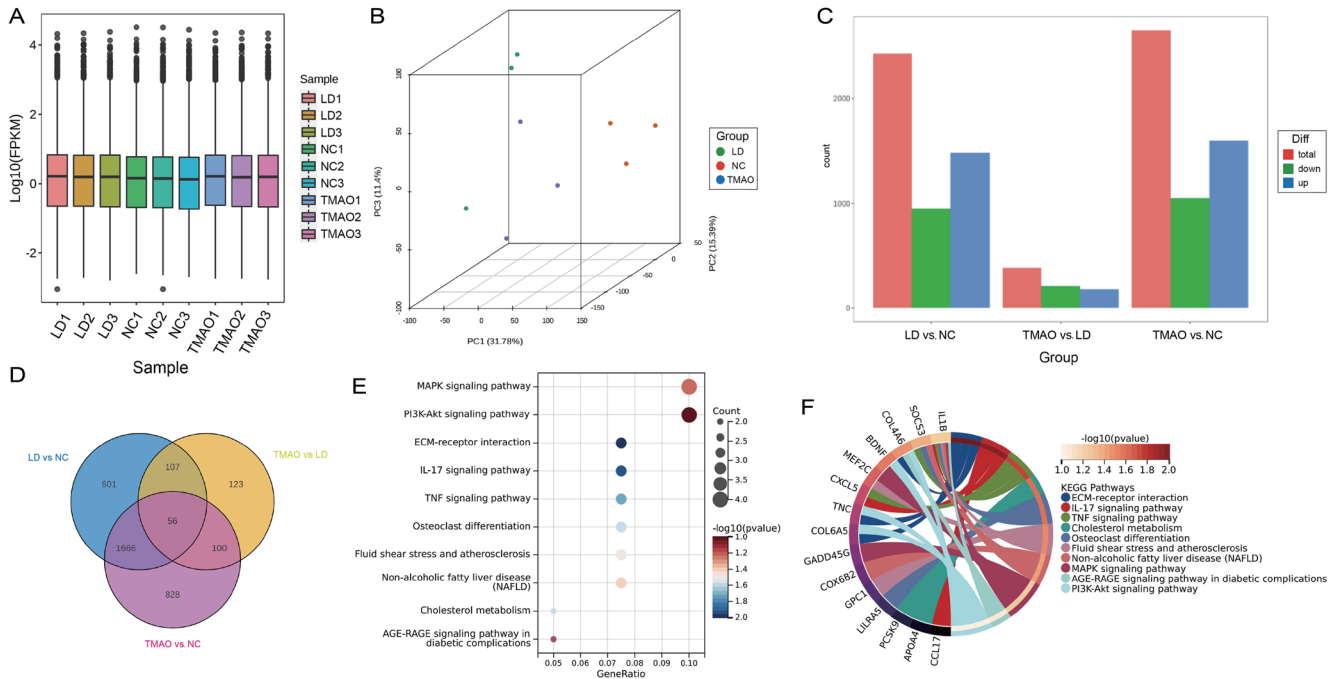


Fig. 2. RNA sequencing of murine liver tissue. (A) Boxplot of FPKM distribution across samples. (B) 3D principal component analysis. (C) Bar chart of differentially expressed genes (DEGs). (D) Venn diagram of DEGs across multiple groups. (E) KEGG enrichment analysis of 100 genes showing significant differences between NC vs. LD+TMAO and LD vs. LD+TMAO, but not between NC and LD. (F) Chord diagram of differentially enriched pathways. LD, lithogenic diet; TMAO, trimethylamine-N-oxide; NC, negative control; KEGG, Kyoto Encyclopedia of Genes and Genomes.

TMAO treatment (Fig. 1E). Hematoxylin and eosin staining revealed that TMAO disrupted hepatic lipid metabolism (Fig. 1D). Furthermore, LD significantly increased cholesterol content and decreased bile acid and phospholipid concentrations in bile, resulting in an elevated CSI. TMAO further increased bile cholesterol content, leading to a further elevation of the CSI (Fig. 1F–I).

Altered cholesterol metabolism in TMAO-treated mice revealed by RNA sequencing

RNA sequencing of hepatic tissue from three randomly selected mice in each group yielded FPKM distribution box plots, showing no significant intergroup differences in overall gene expression levels (Fig. 2A). 3D principal component analysis disclosed significant intragroup similarities and intergroup differences in gene expression (Fig. 2B). Differential gene analysis revealed differentially expressed genes among the NC, LD, and LD+TMAO groups, with 100 genes exhibiting significant differential expression between the NC and LD+TMAO groups, as well as between the LD and LD+TMAO groups, but no significant difference between the NC and LD groups (Fig. 2C, D). We therefore hypothesized that these 100 genes were altered by TMAO. Furthermore, KEGG enrichment analysis of these 100 differentially expressed genes indicated significant enrichment of cholesterol metabolic pathways (Fig. 2E). By selecting the top 10 pathways with the smallest q-values and constructing enrichment analysis and chord diagrams, we identified *PCSK9* and *APOA4* as key regulatory genes in the cholesterol metabolism pathway (Fig. 2F).

TMAO promotes hepatic cholesterol synthesis and efflux

Murine bile flow rate and cholesterol output were significantly higher in the LD group compared to the NC group and further

increased in the LD+TMAO group (Fig. 3A, B). qPCR analysis of murine hepatic tissue disclosed significantly increased mRNA expression levels of the cholesterol biosynthesis-related gene *HMGCR* and the transporter-related genes *ABCG5* and *ABCG8* in the LD group compared to the NC group; this trend was even more pronounced in the LD+TMAO group (Fig. 3C–E). WB analysis of *HMGCR*, *ABCG5*, and *ABCG8* revealed significantly increased expression of these proteins related to cholesterol biosynthesis and transport in the LD group compared to the NC group, and even more significant elevations in the LD+TMAO group (Fig. 3G–J). Immunohistochemistry revealed that the differential expression of *HMGCR*, *ABCG5*, and *ABCG8* was consistent with results obtained from qPCR and WB assays (Fig. 3F).

APOA4 and PCSK9 are key factors in promoting TMAO-mediated lithogenesis

A volcano plot of gene expression revealed decreased *APOA4* and increased *PCSK9* expressions in the LD+TMAO group compared to the LD group (Fig. 4A). qPCR of murine hepatic tissue disclosed no significant differences in *APOA4* and *PCSK9* mRNA levels between the LD and NC groups; however, the LD+TMAO group exhibited significantly decreased *APOA4* and increased *PCSK9* mRNA levels compared to the other two groups (Fig. 4B, C). WB results were consistent with those of the qPCR assays (Fig. 4D–F). GSD patients exhibited significantly lower serum *APOA4* protein levels and higher serum *PCSK9* levels compared to the NC group (Fig. 4G, H).

Inhibited TMAO synthesis suppresses gallstone formation

DMB treatment significantly reduced gallstone formation in the LD group and markedly decreased the mass of intracystic

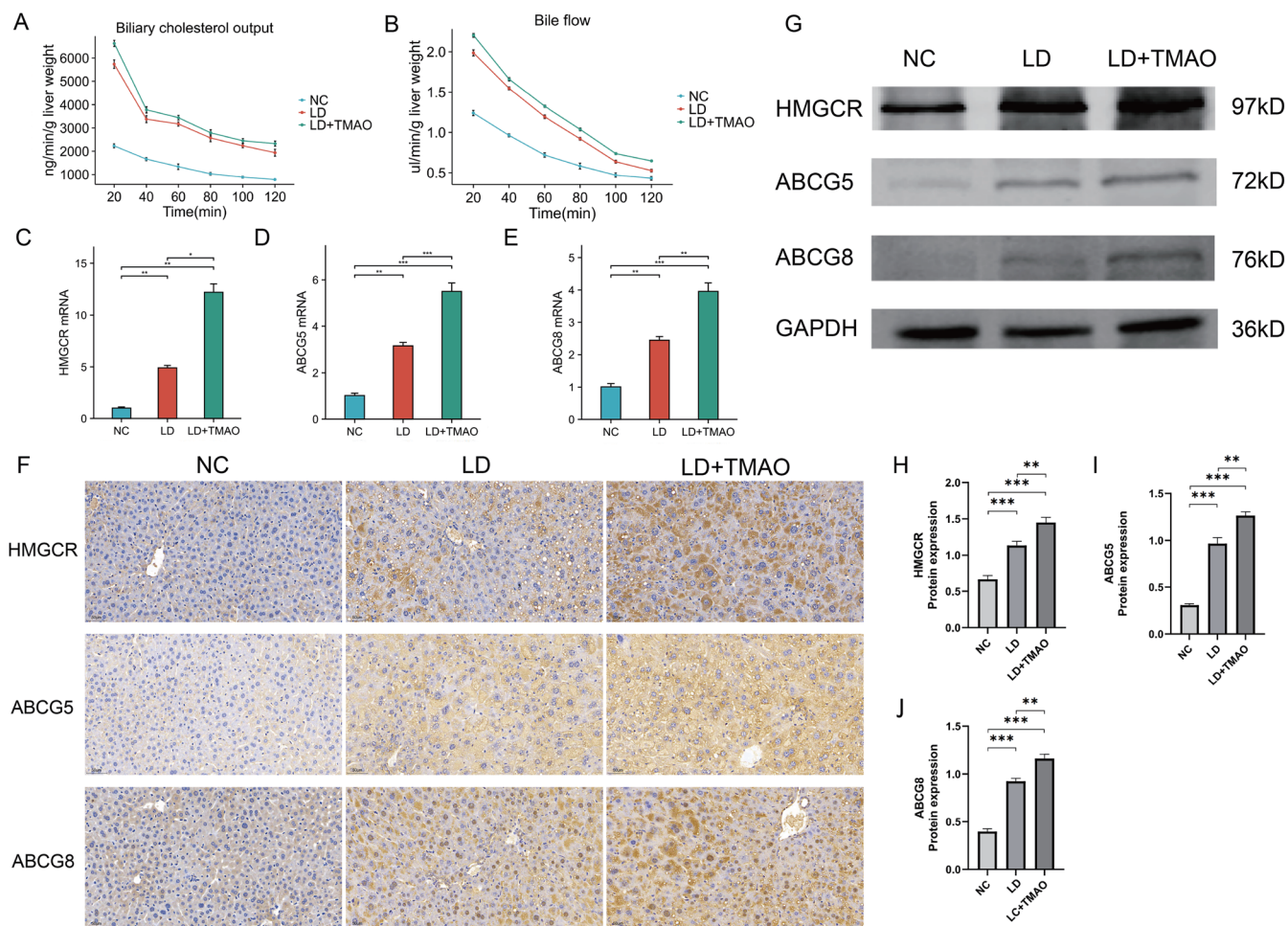


Fig. 3. Changes in cholesterol metabolism in mice following TMAO treatment. (A, B) Total bile flow and cholesterol efflux (n = 3 per group). (C-E) mRNA expression levels of genes related to cholesterol synthesis and transport (n = 3 per group). (F) Immunohistochemical analysis of genes related to cholesterol synthesis and transport. (G-J) Western blot analysis of genes related to cholesterol synthesis and transport (n = 3 per group). *p < 0.05, **p < 0.01, ***p < 0.001. NC, negative control; LD, lithogenic diet; TMAO, trimethylamine-N-oxide; ABCG5, ATP-binding cassette sub-family G member 5; ABCG8, ATP-binding cassette sub-family G member 8; HMGCR, 3-hydroxy-3-methylglutaryl-CoA reductase; GAPDH, glyceraldehyde-3-phosphate dehydrogenase.

solid materials (Fig. 5A, B). Additionally, DMB treatment reduced serum TMAO levels (Fig. 5C). qPCR and immunofluorescence staining revealed that DMB treatment attenuated the LD-induced *APOA4* hypoexpression and *PCSK9* hyperexpression in murine hepatic tissue (Fig. 5D-F). Further rescue experiments confirmed our conclusion that, in a lithogenic background, TMAO promotes gallstone formation by dysregulating the expression of *APOA4* and *PCSK9* proteins.

TMAO regulates APOA4, PCSK9 expressions, and cholesterol metabolism in vitro

PCSK9, *HMGCR*, *ABCG5*, and *ABCG8* mRNA levels were significantly elevated (Fig. 6A-C, E), while *APOA4* mRNA expression was markedly decreased (Fig. 6D) in TMAO-treated compared to control AML12 cells. Increasing TMAO concentrations downregulated *APOA4* expression and upregulated *PCSK9* expression, demonstrating a concentration-dependent effect of TMAO on both *APOA4* and *PCSK9* (Supplementary Fig. 2A, B).

Immunofluorescence staining showed that the fluorescence intensities of *PCSK9*, *HMGCR*, *ABCG5*, and *ABCG8* were significantly higher, while that of *APOA4* was notably

lower in TMAO-treated AML12 cells compared to the control group (Fig. 6F). These findings further demonstrated that TMAO can upregulate the protein expression levels of *PCSK9*, *HMGCR*, *ABCG5*, and *ABCG8*, while downregulating that of *APOA4*, thereby modulating cholesterol metabolism.

TMAO dysregulates cholesterol metabolism by reducing APOA4 and increasing PCSK9 expression, initiating a feedback loop that promotes lithogenesis

To elucidate the specific mechanisms underlying the dysregulation of cholesterol metabolism by TMAO's effects on *APOA4* and *PCSK9* expressions, we conducted an *APOA4* gene functional overexpression study using specific plasmids. The overexpression efficiency of *APOA4* was verified through qPCR (Supplementary Fig. 3A). Protein expression levels of *PCSK9*, *HMGCR*, *ABCG5*, and *ABCG8* were significantly reduced in AML12 cells after *APOA4* overexpression, partially rescuing their TMAO-induced overexpression (Fig. 7A). qPCR analysis of AML12 cells from both NC and *APOA4*-overexpressed groups revealed decreased *PCSK9*, *HMGCR*, *ABCG5*, and *ABCG8* mRNA levels in the *APOA4*-overexpressed group compared to the NC group (Fig. 7B-

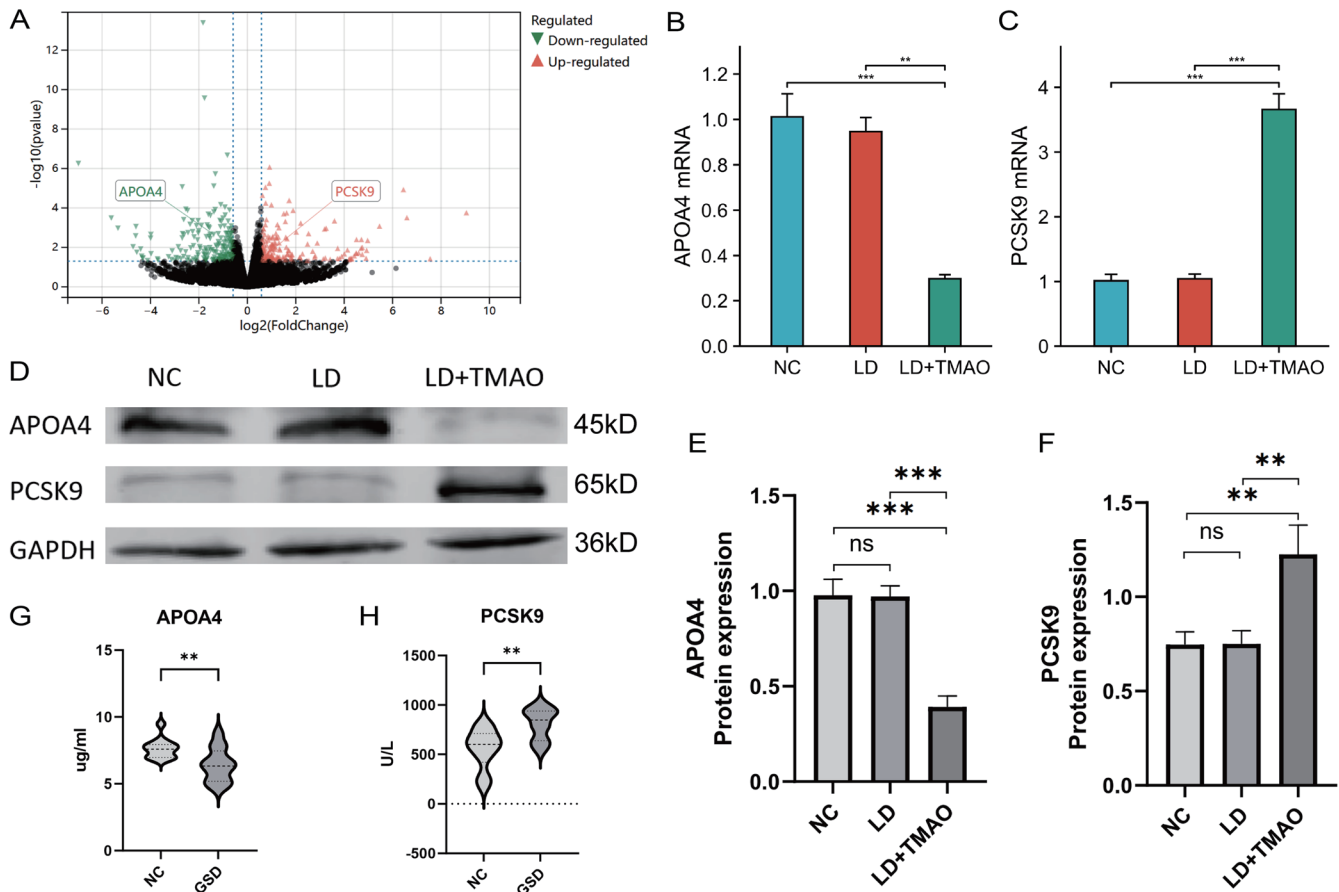


Fig. 4. Changes of APOA4 and PCSK9 expressions in TMAO-induced lithogenesis. (A) Volcano plot of differentially expressed genes from RNA sequencing, showing upregulation of *PCSK9* and downregulation of *APOA4* in the LD+TMAO group compared to the LD group. (B) qRT-qPCR analysis of *APOA4* mRNA expression levels across groups (n = 3 per group). (C) qRT-qPCR analysis of *PCSK9* mRNA levels across groups (n = 3 per group). (D) Western blot analysis of APOA4 and PCSK9 protein levels across groups (n = 3 per group). (E-F). Quantification results of the Western blot analysis using ImageJ. (G, H). Serum APOA4 and PCSK9 levels in patients with cholelithiasis and the control group detected by ELISA. **p < 0.01, ***p < 0.001. LD, lithogenic diet; TMAO, trimethylamine-N-oxide; NC, negative control; APOA4, apolipoprotein A4; PCSK9, proprotein convertase subtilisin/kexin type 9; GSD, gallstone disease; ELISA, enzyme-linked immunosorbent assay.

E). Furthermore, immunofluorescence staining confirmed these findings, demonstrating markedly decreased immunofluorescence intensities of PCSK9, HMGCR, ABCG5, and ABCG8 in the APOA4-overexpressed group, consistent with the qPCR results (Fig. 7F).

Our *PCSK9* gene knockdown study using specific siRNAs verified knockdown efficiencies in AML12 cells via qPCR (Supplementary Fig. 3B). *PCSK9* knockdown significantly reduced protein expression levels of HMGCR, ABCG5, and ABCG8, while *APOA4* expression increased to some extent. Additionally, *PCSK9* knockdown partially rescued TMAO-induced hyperexpression of HMGCR, ABCG5, ABCG8, and *APOA4* hypoexpression (Fig. 7G). qPCR analysis revealed decreased *HMGCR*, *ABCG5*, and *ABCG8*, and increased *APOA4* mRNA levels in the *PCSK9*-knockdown group compared to the NC group (Fig. 7H-K). Immunofluorescence staining further confirmed these findings, demonstrating markedly decreased immunofluorescence intensities of HMGCR, ABCG5, and ABCG8 and a significant increase in *APOA4* immunofluorescence in the *PCSK9*-knockdown group, consistent with the qPCR results (Fig. 7F). Furthermore, we observed a reciprocal feedback loop between *PCSK9* and *APOA4* expression, in which *PCSK9* loss of function promoted *APOA4* expression, and *APOA4* overexpression inhibited *PCSK9* expression.

Discussion

TMAO promotes atherogenesis by upregulating scavenger receptors in macrophages, which promotes cholesterol accumulation and foam cell formation. Furthermore, TMAO enhances inflammation via the MAPK and NF-κB pathways, which have been widely implicated in the progression of atherosclerosis.²⁹ TMAO may also perturb the bile acid profile within the gallbladder.³⁰ However, studies investigating the relationship between TMAO and lithogenesis are scarce. An animal study demonstrated that *FMO3* knockout can prevent obesity and metabolic syndrome.³¹ Additionally, *FMO3* plays a pivotal role in regulating glucose and lipid homeostasis. *FMO3* knockout mice have exhibited significant reductions in hepatic and plasma lipid levels, ketone bodies, glucose, and insulin levels.³² *FMO3* transcription also mediates the activation of the TMA/Fmo3/TMAO pathway, upregulating ABCG5/8, thereby promoting the formation of cholesterol gallstones.³³ These findings are consistent with the conclusions of the current study, which investigated the role of TMAO in lithogenesis. Cholesterol supersaturation in bile is a prerequisite for gallstone formation.³⁴ Located on the membrane of hepatic canaliculi, the ABCG5/8 cholesterol transporter facilitates cholesterol excretion into bile, leading to bile cholesterol supersaturation and gallstone formation.³⁵

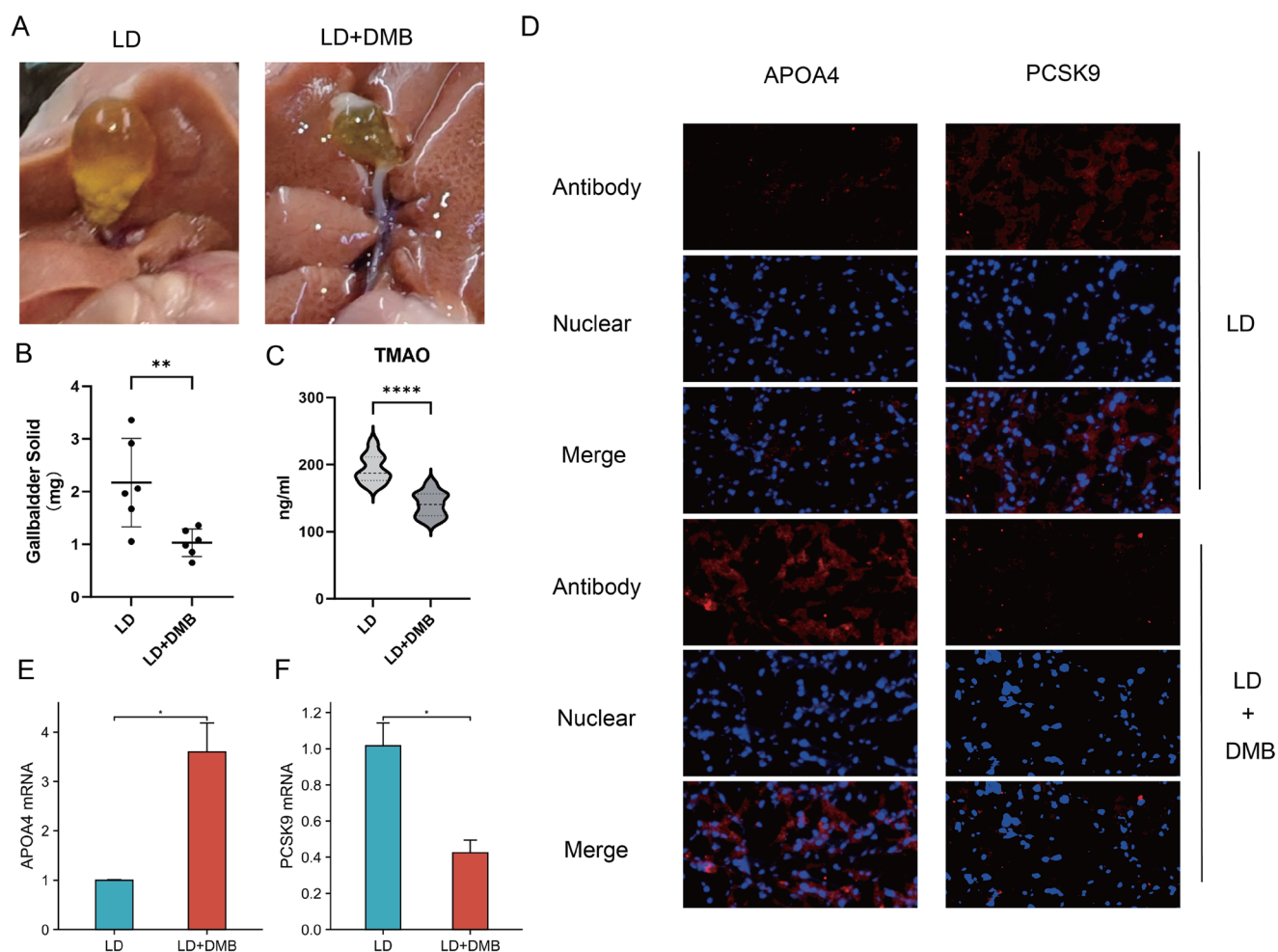


Fig. 5. Effect of TMAO inhibition on lithogenesis and regulation of APOA4 and PCSK9 in a murine model. (A) Lithogenesis in mice from the LD and LD+DMB groups. (B) Weights of solid contents in the gallbladders of mice from each group. (C) Serum TMAO levels in the LD and LD+DMB groups detected by ELISA. (D) Immunofluorescence staining of APOA4 and PCSK9 in hepatic tissues from the LD and LD+DMB groups. (E, F) qRT-qPCR analysis of *APOA4* and *PCSK9* mRNA expression levels in hepatic tissues from the LD and LD+DMB groups. * $p < 0.05$, ** $p < 0.01$, **** $p < 0.0001$. LD, lithogenic diet; DMB, 3,3-dimethyl-1-butanol; TMAO, trimethylamine-N-oxide; ELISA, enzyme-linked immunosorbent assay; APOA4, apolipoprotein A4; PCSK9 proprotein convertase subtilisin/kexin type 9.

Serum TMAO levels were significantly elevated in patients with cholelithiasis compared to the control group. *In vivo*, we observed that TMAO increased the cholesterol content and decreased the bile acid and phospholipid contents of bile, thereby exacerbating gallstone formation in mice. Murine studies by Luo³³ and Chen³⁶ *et al.* also associated plasma TMAO levels with cholelithiasis. This association may be caused by TMAO-induced hypersecretion of bile cholesterol through increased expression of hepatic ABCG5/8, lipoprotein receptor SRB1, and HMGCR, which is consistent with our findings.

Differential and enrichment analyses of our RNA sequencing results from murine hepatic tissue revealed significant enrichment of cholesterol metabolism signaling pathways, with *APOA4* and *PCSK9* identified as key regulatory genes. Notably, the relationship between apolipoproteins and PCSK9 inhibition in cholelithiasis remains controversial and warrants further investigation. As a constituent of high-density lipoprotein, APOA4 may enhance insulin secretion and exert anti-inflammatory, antioxidant, and anti-atherosclerotic effects.³⁷ To our knowledge, no previous studies have demonstrated a direct link between TMAO and APOA4. PCSK9

blocks the recycling of low-density lipoprotein receptors, leading to excessive accumulation of LDL-C,³⁸ which is associated with hyperlipidemia³⁹ and an increased risk of coronary heart disease.⁴⁰ Cross-sectional studies have shown a significant association between TMAO and PCSK9,⁴¹ possibly mediated by IL-8. Furthermore, PCSK9 can promote lithogenesis by inhibiting PPAR α -mediated CYP7A1 expression and preventing the conversion of cholesterol into bile acids.⁴² These findings align with our *in vitro* results. A slight association between PCSK9 and an increased risk of gallstones has been suggested but has not been confirmed by co-localization analysis.⁴³ Inhibition of *PCSK9* promotes hepatic cholesterol biosynthesis, leading to cholesterol oversaturation and gallstone formation.⁴⁴ In contrast, Sanderson *et al.* suggested an association between *APOA4* downregulation and decreased plasma cholesterol,⁴⁵ while Mendelian randomization analyses have speculated that LDL-C reductions caused by PCSK9 or apolipoprotein variants should not affect the risk of symptomatic cholelithiasis.⁴⁶ These observations are incongruent with our conclusions. Specifically, PCSK9 has been associated with apolipoprotein levels,⁴⁷ and specific inhibition of PCSK9 reduces plasma lipoprotein levels.⁴⁸ Inter-

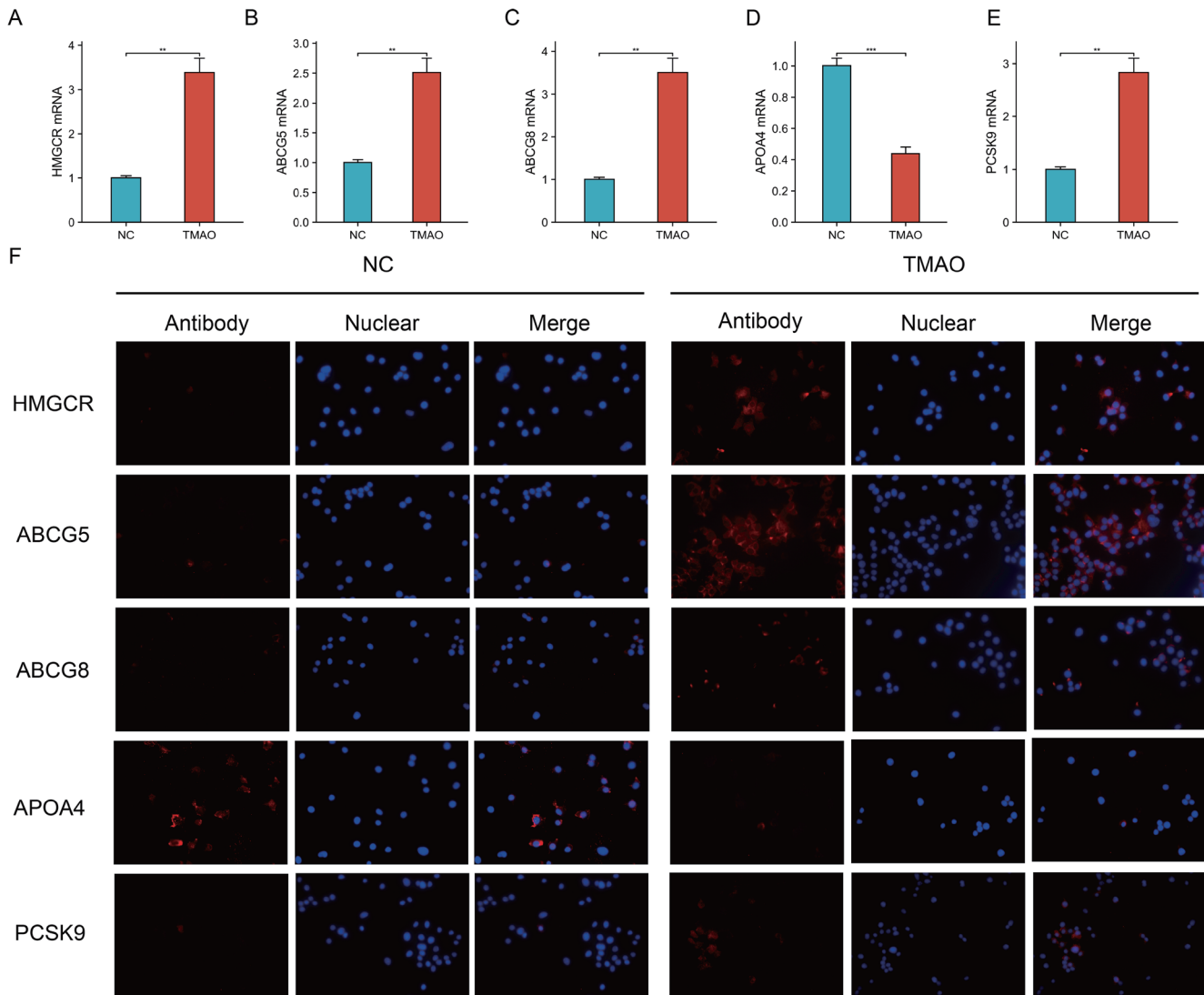


Fig. 6. Effect of TMAO on cholesterol metabolism and APOA4 and PCSK9 expressions *in vitro*. (A–E) APOA4, PCSK9, HMGCR, ABCG5, and ABCG8 mRNA expression levels in TMAO-treated and control AML12 cells (n = 3 per group). (F) Immunofluorescence staining for APOA4, PCSK9, HMGCR, ABCG5, and ABCG8 in cells from each group. ***p* < 0.01, ****p* < 0.001. TMAO, trimethylamine-N-oxide; APOA4, apolipoprotein A4; PCSK9, proprotein convertase subtilisin/kexin type 9; ABCG5, ATP-binding cassette sub-family G member 5; ABCG8, ATP-binding cassette sub-family G member 8; HMGCR, 3-hydroxy-3-methylglutaryl-CoA reductase.

estingly, the relationship between PCSK9 and apolipoprotein levels may vary between ethnic groups.

To further validate the relationship between PCSK9 and APOA4, we conducted gene silencing experiments using siRNA. We knocked down PCSK9 and observed increased APOA4 expression. Interestingly, the insertion of an APOA4 overexpression plasmid decreased PCSK9 expression. We propose that in TMAO-treated murine hepatic tissue, elevated PCSK9 expression inhibits APOA4 expression, while low APOA4 expression further promotes PCSK9 expression, initiating a feedback loop that dysregulates cholesterol metabolism and thereby promoting lithogenesis by increasing cholesterol synthesis and efflux via HMGCR and ABCG5/8, respectively. Consequently, biliary concentrations of cholesterol and bile acids increase and decrease, respectively, thereby promoting the formation of cholesterol gallstones (Fig. 8).

Nevertheless, our understanding of the genetic and molecular basis of lithogenesis is still limited. First, the direct

molecular interactions between TMAO and PCSK9/APOA4, as well as the reciprocal expressions of APOA4 and PCSK9, require further clarification. Furthermore, the collection of liver tissue samples from patients with cholelithiasis to validate our hypothesis would be challenging. Finally, the effectiveness and feasibility of targeting APOA4 and PCSK9 in clinical treatment remain to be demonstrated.

Conclusions

We have discovered that TMAO dysregulates cholesterol metabolism by initiating a feedback loop, upregulating PCSK9 expression, and downregulating APOA4 expression in murine hepatic tissue, thereby promoting gallstone formation. In clinical practice, hyperlipidemia, a risk factor for cardiovascular diseases, also promotes gallstone formation, which should warrant attention. Regulation of blood lipid levels is necessary for patients with cholelithiasis. Targeting PCSK9

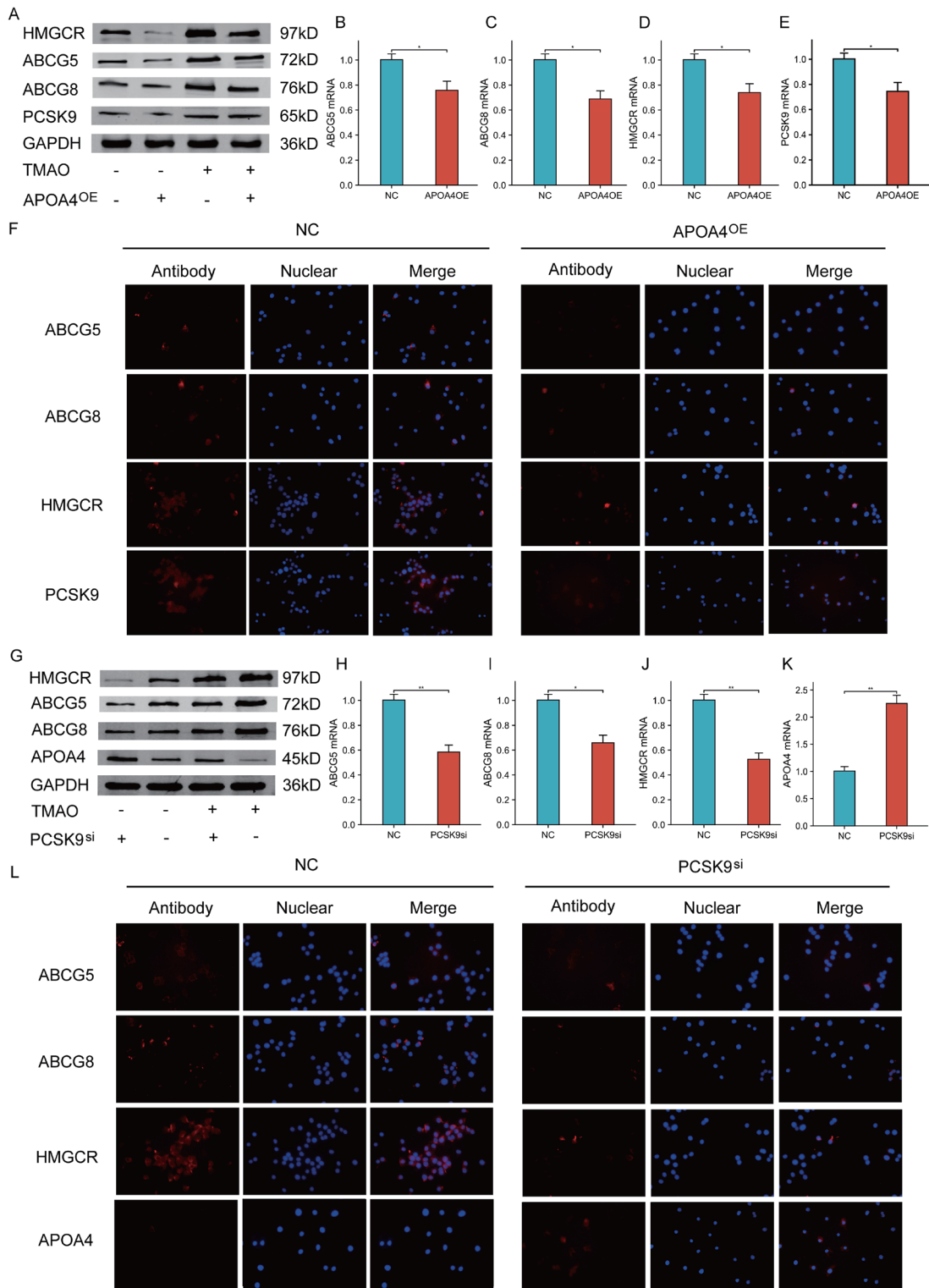


Fig. 7. APOA4-PCSK9 interaction and its alteration by TMAO. (A) WB analysis of PCSK9, HMGCR, ABCG5, and ABCG8 in NC, TMAO-treated, and APOA4-overexpressed cells. (B-E) Changes in *PCSK9*, *HMGCR*, *ABCG5*, and *ABCG8* mRNA levels after *APOA4* overexpression (n = 3 per group). (F) Immunofluorescence staining for intracellular PCSK9, HMGCR, ABCG5, and ABCG8 after *APOA4* overexpression. (G) WB analysis of APOA4, HMGCR, ABCG5, and ABCG8 in NC, TMAO-treated, and PCSK9-knockdown cells. (H-K) Changes in mRNA levels of *PCSK9*, *HMGCR*, *ABCG5*, and *ABCG8* after PCSK9 knockdown (n = 3 per group). (L) Immunofluorescence staining for PCSK9, HMGCR, ABCG5, and ABCG8 in cells after PCSK9 knockdown. **p* < 0.05, ***p* < 0.01. +, positive expression; -, negative expression; TMAO, trimethylamine-N-oxide; APOA4, apolipoprotein A4; PCSK9, proprotein convertase subtilisin/kexin type 9; ABCG5, ATP-binding cassette sub-family G member 5; ABCG8, ATP-binding cassette sub-family G member 8; HMGCR, 3-hydroxy-3-methylglutaryl-CoA reductase; GAPDH, glyceraldehyde-3-phosphate dehydrogenase.

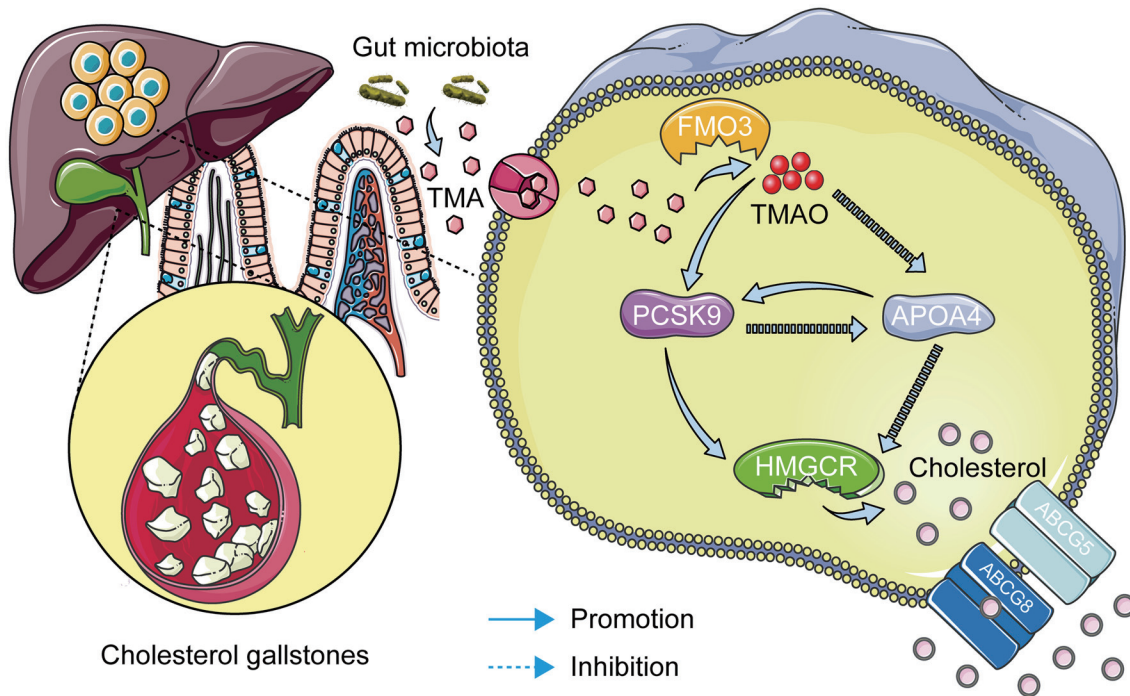


Fig. 8. APOA4-PCSK9 interaction during lithogenesis and effects on cholesterol metabolism and lithogenesis. Gut microbiota produce trimethylamine, which enters the liver via the portal circulation and is primarily oxidized by FMO3 to produce TMAO. TMAO upregulates hepatic PCSK9 gene expression while downregulating APOA4 expression. PCSK9 overexpression inhibits APOA4 expression, while low APOA4 expression further promotes PCSK9 expression, forming a feedback loop that dysregulates cholesterol metabolism. This upregulates cholesterol synthesis by HMGCR and cholesterol efflux by ABCG5/8. Consequently, biliary concentrations of cholesterol and bile acids increase and decrease, respectively, thereby promoting cholesterol gallstone formation. TMAO, trimethylamine-N-oxide; APOA4, apolipoprotein A4; PCSK9, proprotein convertase subtilisin/kexin type 9; ABCG5, ATP-binding cassette sub-family G member 5; ABCG8, ATP-binding cassette sub-family G member 8; FMO3, flavin containing monooxygenase 3; TMA, Trimethylamine.

and APOA4 may represent a promising approach for the prevention and treatment of cholelithiasis.

Acknowledgments

We thank Medjaden Inc. for their assistance in the preparation of this manuscript. The authors sincerely thank all the institutions and individuals who contributed to this research.

Funding

This study was supported by the National Natural Science Foundation of China (No. 82270598), the National Natural Science Foundation of China (No.82100675), and the Open Fund of the Key Laboratory of Hepatosplenic Surgery, Ministry of Education, Harbin, China (No. GPKF202404).

Conflict of interest

The authors have no conflicts of interest related to this publication.

Author contributions

Conceptualization (CS, JY), investigation and formal analysis (CS, JY, ZM), resources (DL, HD, GS), writing – original draft (CS, ZM), writing –review & editing (XM, DX), supervision (XM) and funding acquisition (XM, DX, HS). All authors have read and agreed to the published version of the manuscript.

Ethical statement

The study protocol was approved by the Ethics Committee of The First Affiliated Hospital of Harbin Medical University (No.202322), in strict accordance with the Declaration of Helsinki. This study was conducted in strict accordance with the Guide for the Care and Use of Laboratory Animals formulated by the Ministry of Science and Technology of China in 2006, and all procedures involving animal experiments were conducted according to the regulations of the Institutional Animal Care and Use Committee of The First Affiliated Hospital of Harbin Medical University (No. 2024006).

Data sharing statement

Data supporting the findings of this study are available from the corresponding author upon reasonable request.

References

- [1] Wang X, Yu W, Jiang G, Li H, Li S, Xie L, *et al*. Global Epidemiology of Gallstones in the 21st Century: A Systematic Review and Meta-Analysis. *Clin Gastroenterol Hepatol* 2024;22(8):1586–1595. doi:10.1016/j.cgh.2024.01.051, PMID:38382725.
- [2] Wang Z, Klipfell E, Bennett BJ, Koeth R, Levison BS, Dugar B, *et al*. Gut flora metabolism of phosphatidylcholine promotes cardiovascular disease. *Nature* 2011;472(7341):57–63. doi:10.1038/nature09922, PMID:21475195.
- [3] Jiang S, Shui Y, Cui Y, Tang C, Wang X, Qiu X, *et al*. Gut microbiota dependent trimethylamine N-oxide aggravates angiotensin II-induced hypertension. *Redox Biol* 2021;46:102115. doi:10.1016/j.redox.2021.102115, PMID:34474396.
- [4] Wang M, Li XS, Wang Z, de Oliveira Otto MC, Lemaitre RN, Fretts A, *et al*. Trimethylamine N-oxide is associated with long-term mortality risk: the multi-ethnic study of atherosclerosis. *Eur Heart J* 2023;44(18):1608–1618. doi:10.1093/eurheartj/ehad089, PMID:36883587.

- [5] Heianza Y, Ma W, DiDonato JA, Sun Q, Rimm EB, Hu FB, *et al*. Long-Term Changes in Gut Microbial Metabolite Trimethylamine N-Oxide and Coronary Heart Disease Risk. *J Am Coll Cardiol* 2020;75(7):763–772. doi:10.1016/j.jacc.2019.11.060, PMID:32081286.
- [6] Zhu W, Romano KA, Li L, Buffa JA, Sangwan N, Prakash P, *et al*. Gut microbes impact stroke severity via the trimethylamine N-oxide pathway. *Cell Host Microbe* 2021;29(7):1199–1208.e5. doi:10.1016/j.chom.2021.05.002, PMID:34139173.
- [7] Benson TW, Conrad KA, Li XS, Wang Z, Helsley RN, Schugar RC, *et al*. Gut Microbiota-Derived Trimethylamine N-Oxide Contributes to Abdominal Aortic Aneurysm Through Inflammatory and Apoptotic Mechanisms. *Circulation* 2023;147(14):1079–1096. doi:10.1161/CIRCULATIONAHA.122.060573, PMID:37011073.
- [8] Mo X, Cheng R, Shen L, Sun Y, Wang P, Jiang G, *et al*. High-fat diet induces sarcopenic obesity in natural aging rats through the gut-trimethylamine N-oxide-muscle axis. *J Adv Res* 2024. doi:10.1016/j.jare.2024.05.015.
- [9] Huang Y, Wu Y, Zhang Y, Bai H, Peng R, Ruan W, *et al*. Dynamic Changes in Gut Microbiota-Derived Metabolite Trimethylamine-N-Oxide and Risk of Type 2 Diabetes Mellitus: Potential for Dietary Changes in Diabetes Prevention. *Nutrients* 2024;16(11):1711. doi:10.3390/nu16111711, PMID:38892643.
- [10] Chen Y, Yang C, Dai Q, Tan J, Dou C, Luo F. Gold-nanosphere mitigates osteoporosis through regulating TMAO metabolism in a gut microbiota-dependent manner. *J Nanobiotechnology* 2023;21(1):125. doi:10.1186/s12951-023-01872-9, PMID:37041523.
- [11] Wu K, Yuan Y, Yu H, Dai X, Wang S, Sun Z, *et al*. The gut microbial metabolite trimethylamine N-oxide aggravates GVHD by inducing M1 macrophage polarization in mice. *Blood* 2020;136(4):501–515. doi:10.1182/blood.2019003990, PMID:32291445.
- [12] Wang M, Tang WHW, Li XS, de Oliveira Otto MC, Lee Y, Lemaitre RN, *et al*. The Gut Microbial Metabolite Trimethylamine N-oxide, Incident CKD, and Kidney Function Decline. *J Am Soc Nephrol* 2024;35(6):749–760. doi:10.1681/ASN.000000000000344, PMID:38593157.
- [13] Luo T, Guo Z, Liu D, Guo Z, Wu Q, Li Q, *et al*. Deficiency of PSRC1 accelerates atherosclerosis by increasing TMAO production via manipulating gut microbiota and flavin monooxygenase 3. *Gut Microbes* 2022;14(1):2077602. doi:10.1080/19490976.2022.2077602, PMID:35613310.
- [14] Chen S, Henderson A, Petriello MC, Romano KA, Gearing M, Miao J, *et al*. Trimethylamine N-Oxide Binds and Activates PERK to Promote Metabolic Dysfunction. *Cell Metab* 2019;30(6):1141–1151.e5. doi:10.1016/j.cmet.2019.08.021, PMID:31543404.
- [15] Wang D, Ye A, Jiang N. The role of bacteria in gallstone formation. *Folia Microbiol (Praha)* 2024;69(1):33–40. doi:10.1007/s12223-024-01131-w, PMID:38252338.
- [16] Hu H, Shao W, Liu Q, Liu N, Wang Q, Xu J, *et al*. Gut microbiota promotes cholesterol gallstone formation by modulating bile acid composition and biliary cholesterol secretion. *Nat Commun* 2022;13(1):252. doi:10.1038/s41467-021-27758-8, PMID:35017486.
- [17] Amigo L, Castro J, Miquel JF, Zanolungo S, Young S, Nervi F. Inactivation of hepatic microsomal triglyceride transfer protein protects mice from diet-induced gallstones. *Gastroenterology* 2006;131(6):1870–1878. doi:10.1053/j.gastro.2006.08.029, PMID:17064699.
- [18] Lai Y, Tang H, Zhang X, Zhou Z, Zhou M, Hu Z, *et al*. Trimethylamine-N-Oxide Aggravates Kidney Injury via Activation of p38/MAPK Signaling and Upregulation of HuR. *Kidney Blood Press Res* 2022;47(1):61–71. doi:10.1159/000519603, PMID:34788763.
- [19] Wang J, Gao Y, Ren S, Li J, Chen S, Feng J, *et al*. Gut microbiota-derived trimethylamine N-Oxide: a novel target for the treatment of preclampsia. *Gut Microbes* 2024;16(1):2311888. doi:10.1080/19490976.2024.2311888, PMID:38351748.
- [20] Matsumoto K, Imasato M, Yamazaki Y, Tanaka H, Watanabe M, Eguchi H, *et al*. Claudin 2 deficiency reduces bile flow and increases susceptibility to cholesterol gallstone disease in mice. *Gastroenterology* 2014;147(5):1134–45.e10. doi:10.1053/j.gastro.2014.07.033, PMID:25068494.
- [21] Carey MC. Critical tables for calculating the cholesterol saturation of native bile. *J Lipid Res* 1978;19(8):945–955. PMID:731129.
- [22] Melko M, Winczura K, Rouvière JO, Oborská-Oplová M, Andersen PK, Heick Jensen T. Mapping domains of ARS2 critical for its RNA decay capacity. *Nucleic Acids Res* 2020;48(12):6943–6953. doi:10.1093/nar/gkaa445, PMID:32463452.
- [23] Chen S, Zhou Y, Chen Y, Gu J. fastp: an ultra-fast all-in-one FASTQ pre-processor. *Bioinformatics* 2018;34(17):i884–i890. doi:10.1093/bioinformatics/bty560, PMID:30423086.
- [24] Yu J, Meng Z, Liu X, Zheng Y, Xue D, Hao C, *et al*. Lipopolysaccharide in Bile Promotes the Neutrophil Extracellular Traps-Induced Gallstone Formation by Activating the Gallbladder Immune Barrier. *Immunotargets Ther* 2024;13:789–803. doi:10.2147/ITT.S495095, PMID:39712952.
- [25] Nguyen HX, Kirkton RD, Bursac N. Generation and customization of bio-synthetic excitable tissues for electrophysiological studies and cell-based therapies. *Nat Protoc* 2018;13(5):927–945. doi:10.1038/nprot.2018.016, PMID:29622805.
- [26] Gupta N, Wu CH, Wu GY. Targeted transplantation of mitochondria to hepatocytes. *Hepat Med* 2016;8:115–134. doi:10.2147/HMER.S116852, PMID:27942238.
- [27] Kondo H, Ratcliffe CDH, Hooper S, Ellis J, MacRae JI, Hennequart M, *et al*. Single-cell resolved imaging reveals intra-tumor heterogeneity in glycolysis, transitions between metabolic states, and their regulatory mechanisms. *Cell Rep* 2021;34(7):108750. doi:10.1016/j.celrep.2021.108750, PMID:33596424.
- [28] Clayton ZE, Tan RP, Miravet MM, Lennartsson K, Cooke JP, Bursill CA, *et al*. Induced pluripotent stem cell-derived endothelial cells promote angiogenesis and accelerate wound closure in a murine excisional wound healing model. *Biosci Rep* 2018;38(4):BSR20180563. doi:10.1042/BSR20180563, PMID:29976773.
- [29] He H, Lian X, Tang Z. Research progress of trimethylamine-N-oxide in the pathogenesis of atherosclerosis. *Zhong Nan Da Xue Xue Bao Yi Xue Ban* 2017;42(8):986–990. doi:10.11817/j.issn.1672-7347.2017.08.018, PMID:28872093.
- [30] Yang JY, Zhang TT, Yu ZL, Wang CC, Zhao YC, Wang YM, *et al*. Taurine Alleviates Trimethylamine N-Oxide-Induced Atherosclerosis by Regulating Bile Acid Metabolism in ApoE(-/-) Mice. *J Agric Food Chem* 2022;70(18):5738–5747. doi:10.1021/acs.jafc.2c01376, PMID:35486890.
- [31] Schugar RC, Shih DM, Warriar M, Helsley RN, Burrows A, Ferguson D, *et al*. The TMAO-Producing Enzyme Flavin Monooxygenase 3 Regulates Obesity and the Beiging of White Adipose Tissue. *Cell Rep* 2017;19(12):2451–2461. doi:10.1016/j.celrep.2017.05.077, PMID:28636934.
- [32] Shih DM, Wang Z, Lee R, Meng Y, Che N, Charugundla S, *et al*. Flavin containing monooxygenase 3 exerts broad effects on glucose and lipid metabolism and atherosclerosis. *J Lipid Res* 2015;56(1):22–37. doi:10.1194/jlr.M051680, PMID:25378658.
- [33] Luo M, Chen P, Tian Y, Rigzin N, Sonam J, Shang F, *et al*. Hif-1 α expression targets the TMA/Fmo3/TMAO axis to participate in gallbladder cholesterol stone formation in individuals living in plateau regions. *Biochim Biophys Acta Mol Basis Dis* 2024;1870(5):167188. doi:10.1016/j.bbdis.2024.167188, PMID:38657913.
- [34] Di Ciaula A, Wang DQ, Portincasa P. An update on the pathogenesis of cholesterol gallstone disease. *Curr Opin Gastroenterol* 2018;34(2):71–80. doi:10.1097/MOG.0000000000000423, PMID:29283909.
- [35] Jiang ZY, Parini P, Eggertsen G, Davis MA, Hu H, Suo GJ, *et al*. Increased expression of LXR alpha, ABCG5, ABCG8, and SR-BI in the liver from normolipidemic, nonobese Chinese gallstone patients. *J Lipid Res* 2008;49(2):464–472. doi:10.1194/jlr.M700295-JLR200, PMID:18007013.
- [36] Chen Y, Weng Z, Liu Q, Shao W, Guo W, Chen C, *et al*. FMO3 and its metabolite TMAO contribute to the formation of gallstones. *Biochim Biophys Acta Mol Basis Dis* 2019;1865(10):2576–2585. doi:10.1016/j.bbdis.2019.06.016, PMID:31251986.
- [37] Qu J, Ko CW, Tso P, Bhargava A. Apolipoprotein A-IV: A Multifunctional Protein Involved in Protection against Atherosclerosis and Diabetes. *Cells* 2019;8(4):319. doi:10.3390/cells8040319, PMID:30959835.
- [38] Solanki A, Bhatt LK, Johnston TP. Evolving targets for the treatment of atherosclerosis. *Pharmacol Ther* 2018;187:1–12. doi:10.1016/j.pharmthera.2018.02.002, PMID:29414673.
- [39] Lu X, Li J, Li H, Chen Y, Wang L, He M, *et al*. Coding-sequence variants are associated with blood lipid levels in 14,473 Chinese. *Hum Mol Genet* 2016;25(18):4107–4116. doi:10.1093/hmg/ddw261, PMID:27516387.
- [40] Willer CJ, Sanna S, Jackson AU, Scuteri A, Bonnycastle LL, Clarke R, *et al*. Newly identified loci that influence lipid concentrations and risk of coronary artery disease. *Nat Genet* 2008;40(2):161–169. doi:10.1038/ng.76, PMID:18193043.
- [41] Baginski AM, Farmer N, Baumer Y, Wallen GR, Powell-Wiley TM. Interleukin-8 (IL-8) as a Potential Mediator of an Association between Trimethylamine N-Oxide (TMAO) and Proprotein Convertase Subtilisin/Kexin Type 9 (PCSK9) among African Americans at Risk of Cardiovascular Disease. *Metabolites* 2022;12(12):1196. doi:10.3390/metabo12121196, PMID:36557234.
- [42] Chen Z, Shao W, Li Y, Zhang X, Geng Y, Ma X, *et al*. Inhibition of PCSK9 prevents and alleviates cholesterol gallstones through PPAR α -mediated CYP7A1 activation. *Metabolism* 2024;152:155774. doi:10.1016/j.metabol.2023.155774, PMID:38191052.
- [43] Chen L, Qiu W, Sun X, Gao M, Zhao Y, Li M, *et al*. Novel insights into causal effects of serum lipids and lipid-modifying targets on cholelithiasis. *Gut* 2024;73(3):521–532. doi:10.1136/gutjnl-2023-330784, PMID:37945330.
- [44] Ioannou GN, Lee SP, Linsley PS, Gersuk V, Yeh MM, Chen YY, *et al*. Pcsk9 Deletion Promotes Murine Nonalcoholic Steatohepatitis and Hepatic Carcinogenesis: Role of Cholesterol. *Hepatology Commun* 2022;6(4):780–794. doi:10.1002/hep4.1858, PMID:34816633.
- [45] Sanderson LM, Boekschoten MV, Desvergne B, Müller M, Kersten S. Transcriptional profiling reveals divergent roles of PPAR α and PPAR β /delta in regulation of gene expression in mouse liver. *Physiol Genomics* 2010;41(1):42–52. doi:10.1152/physiolgenomics.00127.2009, PMID:20090909.
- [46] Stender S, Frikke-Schmidt R, Bønn M, Nordestgaard BG, Tybjaerg-Hansen A. Low-density lipoprotein cholesterol and risk of gallstone disease: a Mendelian randomization study and meta-analyses. *J Hepatol* 2013;58(1):126–133. doi:10.1016/j.jhep.2012.08.013, PMID:22922093.
- [47] Tavori H, Christian D, Minnier J, Plubell D, Shapiro MD, Yeang C, *et al*. PCSK9 Association With Lipoprotein(a). *Circ Res* 2016;119(1):29–35. doi:10.1161/CIRCRESAHA.116.308811, PMID:27121620.
- [48] Ying Q, Chan DC, Pang J, Marcovina SM, Barrett PHR, Watts GF. PCSK9 inhibition with alirocumab decreases plasma lipoprotein(a) concentration by a dual mechanism of action in statin-treated patients with very high apolipoprotein(a) concentration. *J Intern Med* 2022;291(6):870–876. doi:10.1111/joim.13457, PMID:35112754.